# Screening for adsorptions of Calbindin $D_{9k}$ and Monellin proteins to Silica nanoparticles

Nora Klynning
Supervisor: Martin Lundqvist
Department of Biology, Lund University, MOBK01, HT2016
nat13nkl@student.lu.se

**Abstract**
Although nanoparticles (NPs) are very small, their field in science is currently growing very large. There are several biological, medical and technical applications possible for NPs when bound to proteins. Protein-NP interactions are difficult to predict and therefore a lot of fundamental research is yet to be completed. This study is an attempt to contribute with the aim to explore the interaction between two different proteins with three different sizes of silica NPs. By fluorescence spectroscopy light have been shone on silica NPs and their interactive behavior in combination with three different mutations of the two proteins calbindin $D_{9k}$ and monellin respectively. The fluorescence intensity was measured with two different fluorophores; ANS and NR. The study considers six different scenarios of interaction to be possible. Dynamic light scattering measurements were carried out to complement the fluorescence screening results. Interaction appear to be occurring, particularly for the specific combination of the positively charged (+8) mutation of monellin and silica NP, which also indicate on protein concentration dependence. The NP size appear to have an impact on the concentration limits for (+8) mutation of monellin. The results of the experiments also indicate that ANS is a more suitable fluorophore than NR for fluorescence measurements on silica NPs.

## 1. Introduction

Having knowledge about the world around us, small as big, has always been of interest for humankind. The smallest of worlds was first explored in the early 1980s (Lindsay, 2010) as the field of nanoscience took off. Nano dimension means one billionth of a meter and accordingly, nanoparticles (NPs) are defined as particles with at least one external dimension of 1–100 nanometers (nm) or less (Rauscher et al., 2013). NPs are always present (Napierska et al., 2010) and even though it is not visible to the human eye they may interact with everything they come across.

For instance, NPs will, when in contact with biomolecules such as proteins, most likely interact; either bind or not. There are several reasons to study interactions between nanoparticles and comparable sizes of biomolecules, e.g. proteins. Biological, medical and technical applications of NPs depend on interactions between NPs and proteins (Nasir et al., 2015).

Human interactions are dependent on personality and characteristics. Obviously, both NPs and proteins lack personality traits, however, they both carry characteristics such as size, charge and hydrophobicity. These and possibly other characteristics may all play important roles in protein-NP interactions (Huang et al., 2013). NPs are particularly interesting since they have the same size scope as most biological processes in the human body. If – or when – biological processes go wrong, the potentially best possible tools to use in order to recognize and hopefully heal the deficiency involve NPs (Rosi and Mirkin, 2005).

Depending on the size, shape and surface modification of the NP the interactions will differ. Characteristics such as charge and hydrophobicity of the interacting protein will also influence the outcome. If a protein binds to a NP, a conformational change of the protein can occur and, hence, the protein's function will most likely be influenced. This may trigger unwanted biological responses *in vivo* (Lundqvist, Sethson and Jonsson, 2004). The risk this

entails, or perhaps the possibilities, is yet to be discovered and therefore protein-NP interactions are of great interest to study.

In order to make better predictions about protein-NP interactions, fundamental research for specific combinations is needed. In this study the specific combinations of silica NPs and the two proteins calbindin $D_{9k}$ and monellin have been investigated. Characteristic for silica NPs is their high negative surface charge (Lundqvist et al., 2006). The proteins used in this study had three different mutations. Mutations of calbindin $D_{9k}$ used were M0, M11 and M56 and mutations of Monellin were (-2), (+2) and (+8). Both proteins have been used in previous work at the laboratory where this experiment was held and thus appropriate to use. The two proteins are both intriguing, however in different ways. Calbindin $D_{9k}$ is a calcium binding protein that is highly inert as it has no confirmed interaction partners based on protein array studies (O'Connell et al., 2011). The different monellin mutations have different surface properties due to their different charge and are therefore very applicable to this experiment.

## 2. Methods

Four different methods have been used in this study. Dialysis and absorbance measurements were needed as preparatory steps for the main two investigational methods that were fluorescence measurements and Dynamic Light Scattering.

### *2.1 Dialysis*

Dialysis works by diffusion of solutes and filtration of fluid across a semi-permeable membrane against a solution with desired properties (Mosby's dictionary of medicine, nursing & health professions, 2006). This was done on the NPs as a preparation step ahead of the main measurements of the experiment. For the NPs used in this experiment a TRIS-buffer pH 8.4 was used which gives the NPs an environment where they have colloidal stability. It also purifies the particles, removes sodium ions, and it lowers the pH value which is of importance as high pH value would denaturate the proteins later used in the experiment.

### *2.2 $A^{280}$ absorbance spectroscopy*

This method is used to measure the absorbance of a substance by first illuminating a sample cell with light of a predetermined intensity, $I_0$, whereafter the light output, $I$, is measured. Thus, the absorbance, $A$, of the sample cell content can be determined. $I_0$ was set to 280 nm in this experiment. Absorbance is defined as:

$$A = \log (I_0/I) \qquad (1)$$

Absorbance relates to the concentration through Lambert-Beer law (Daintith, 2008):

$$A = \varepsilon \cdot c \cdot l \qquad (2)$$

$\varepsilon$ is the extinction coefficient specific for each protein and wavelength, $c$ is the light-absorbing substance concentration and $l$ is the length of the light path. The $\varepsilon$-value for monellin and calbindin $D_{9k}$ is 14600 $M^{-1}cm^{-1}$ and 1490 $M^{-1}cm^{-1}$ respectively (Nasir et al., 2015). This method was used to obtain protein concentration values to prepare stock solutions.

### *2.3 Fluorescence spectroscopy*

In this experiment fluorescence spectroscopy was used to measure interaction between NPs and proteins. To measure fluorescence intensity ($I_F$), a fluorophore must be present. A fluorophore is a molecule that, upon exposure to light, can re-emit the light. The wavelengths

for emission are characteristic of the fluorophore and dependent on its chemical environment. Two different fluorophores have been used in this study; 8-Anilino-1-naphthalenesulfonic acid ammonium salt (ANS) and Nile Red (NR). ANS is negatively charged and is sensitive to the polarity of the local environment and light emission from the fluorophore is associated with the hydrophobicity of proteins. Likewise, NR also reports on accessible hydrophobic surfaces (Assarsson, 2014). To obtain optimal signal interpretation qualities, emission filters in the fluorospectrometer were set to 460 and 475 for ANS and 590, 630 and 660 for NR.

The output of the fluorescence screenings can be described by three possible scenarios (Nasir et al., 2015) which are presented in Figure 1. NPs are illustrated in blue, fluorophores in red and proteins in green. Depending on whether the fluorophore adsorbs to the NP or not, the scenarios can be divided into two different main sections (A and B).

Section A: no fluorophore adsorption to the NP.

1a: The protein binds to the particles and therefore the fluorophores that were bound to the protein are released into the surrounding volume. The $I_F$ is lower for NP-protein combination than for the sum of the $I_F$ of NP and protein controls ($I_{F\ total} < I_{F\ protein} + I_{F\ NP}$).

2a: The protein binds to the NPs and consequently undergoes conformational changes leading to exposure of hydrophobic patches to which the fluorophore can bind. The $I_F$ is higher for NP-protein combination compared to the sum of the $I_F$ of NP and protein controls ($I_{F\ total} > I_{F\ protein} + I_{F\ NP}$).

3a: The protein does not adsorb to the NP or the NP-protein complex. The $I_F$ of the NP-protein combination is equal to the sum of the $I_F$ of NP and protein controls ($I_{F\ total} = I_{F\ protein} + I_{F\ NP}$).

Section B: the fluorophore adsorbs to the NP.

1b: The protein has higher affinity for the NP surface than the fluorophore leading to displacement of the fluorophore from the NP surface. The $I_F$ is lower in the NP-protein sample than for the sum of the $I_F$ of NP and protein controls ($I_{F\ total} < I_{F\ protein} + I_{F\ NP}$).

2b: Protein and fluorophore both adsorb to the NP surface. Due to conformational changes, hydrophobic patches of the protein are exposed to the surrounding volume. The $I_F$ is higher in the NP-protein sample compared to the sum of the $I_F$ of NP and protein controls ($I_{F\ total} > I_{F\ protein} + I_{F\ NP}$).

3b: The protein has lower affinity to the NP surface than the already adsorbed fluorophore. The $I_F$ of the NP-protein sample is the same as for the sum of the $I_F$ of NP and protein controls ($I_{F\ total} = I_{F\ protein} + I_{F\ NP}$).

*2.4 Dynamic Light Scattering*

Dynamic Light Scattering (DLS) is a commonly used technique for NP size determination in suspension (Shang, Nienhaus and Nienhaus, 2014). The technique is used to analyze particles in solution through variation in scattering intensity. A laser beam is projected through the sample to measure the scattering at a pre-defined angle. The properties of the sample results in various light scattering patterns. For instance, smaller particles cause a greater fluctuation in scattering intensity compared to larger particles. By applying a mathematical function to the variation in intensity, the distribution of the radius of the particles can be calculated. Measurement reliability is associated with homogeneity of the solution (Assarsson, 2014). A DLS plate reader (DynaPro Plate Reader II, Wyatt Technology, Santa Barbara, CA) operating with a 158° scattering angle at 25° C was used throughout this experiment.

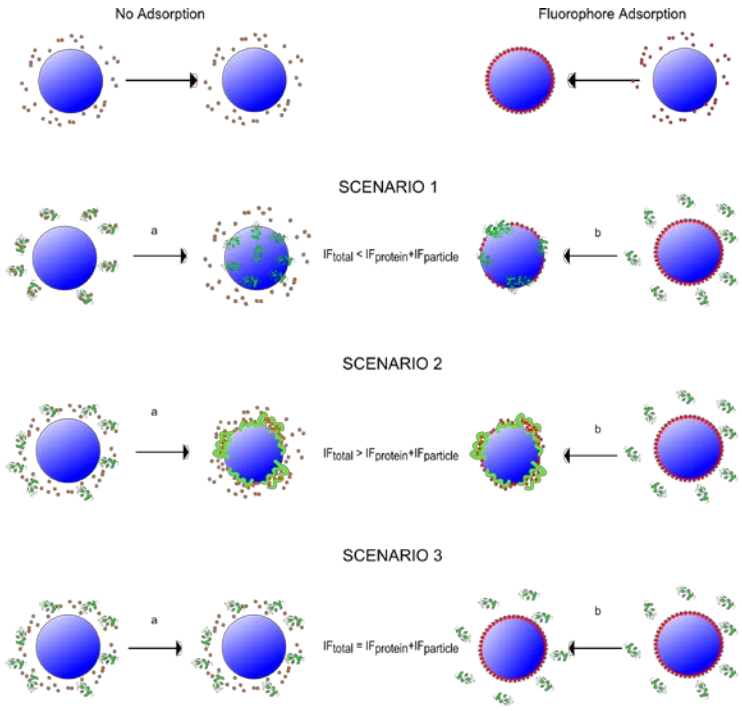


*Figure 1. Schematic illustration of the three possible interaction scenarios between nanoparticles (blue) and proteins (green) in presence of fluorophore (red) (Lundqvist, 2016).*

## 3. Materials

### *3.1 Buffers*

10mM HEPES buffer pH 7.4 was used throughout all experiments for all samples. TRIS buffer pH 8.4 was used for dialysis, neutralized with HCl to reach desired pH value. The pH value was set by using a pH-meter.

### *3.2 NPs*

Silica NPs of three different sizes (S1, S2 and S3) were used with estimated diameters of 20, 35 and 100 nm respectively. They were obtained from EKA NOBEL and were received in a strong basic solution (≈ pH 11-13). All particles were filtered through a syringe filter and then dialyzed against TRIS buffer. DLS of different particle concentrations in HEPES-buffer was performed to obtain a control value of their sizes. To ensure the same particle area exposure to the proteins, information about their concentration and surface area was received from supervisor.

### *3.3 Proteins*

Three different variants of two different proteins were used to measure NP-protein interaction; bovine calbindin $D_{9k}$ wild type M0 and mutations M11 and M56, and monellin mutations (-2), (+2) and (+8). The proteins were expressed at Lund University by recombination in *Escherichia coli*. The calbindin $D_{9k}$ mutations were all negatively charged. Monellin mutation (-2) had a negative charge of -2 while (+2) and (+8) were positively charged +2 and +8 as their names indicate. Protein stock solutions were made by taking 1.5 mg dry frozen proteins dissolved in 1 ml HEPES-buffer and centrifuged. The concentration was checked by using absorbance measured with a spectrophotometer.

*3.4 Fluorophores*

The fluorophores 8-Anilino-1-naphthalenesulfonic acid ammonium salt (ANS) and Nile Red (NR) were used to detect fluorescens. Neither ANS nor NR report on charge, only hydrophobicity (Assarsson, 2014). ANS was used as received without further purification and was dissolved in water to reach a stock concentration of 1.3 mg/ml which was diluted to a final concentration of 0.195 mg/ml in each well. NR was dissolved in dimethyl sulfoxide (DMSO) to get a stock concentration of 100 μM. To limit the amount of DMSO in the sample wells, the final NR concentration was set to 1 μM.

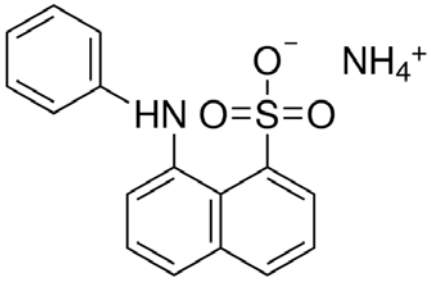


*Figure 2. Chemical structure of ANS (Sigma-Aldrich).*

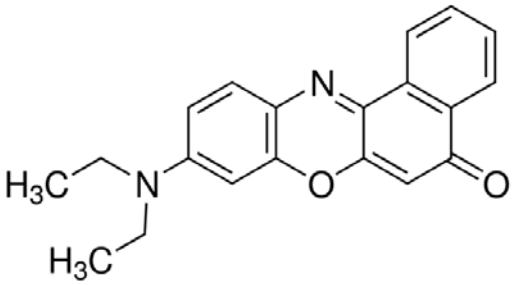


*Figure 3. Chemical structure of NR (Sigma-Aldrich).*

*3.5 Samples*

Stock solutions for each sample were mixed in the following order: buffer, fluorophore, NP and protein. Three replicates of each sample were made with the final volume of 100 μl in each well. The stock solutions therefore had a volume of 400 μl to be sufficient for all replicates. The full screenings had a protein concentration range between 0.02 mg/ml and 1.4 mg/ml in the samples. The concentration of S1, S2 and S3 in each sample was 0.13, 0.20 and 0.56 mg/ml respectively. The samples were measured in plates of 96 well half-area of black polystyrene with clear bottom and non-binding surface for all screenings.

*3.6 Test runs*

A first test run was done to obtain well-adjusted gain settings. This was followed by full screenings with ANS and NR respectively. The plate plans for these test runs are illustrated in Appendix, Figure 7 and 8. An additional test run was performed to more accurately examine the NP-protein interaction of monellin (+8) mutation with a concentration range of 0.02 – 0.1 mg/ml, plate plan illustrated in Appendix, Figure 9. DLS measurements were performed after each test run.

**4. Results**

*4.1 Fluorescence measurements with ANS*

Results from fluorescence measurements with ANS are presented in Figure 4, and DLS data from the same test run is presented in Table 1. All diagrams except that of (+8) mutation of monellin in Figure 2 show graphs with similar levels of fluorescence intensity. Fluorescence intensity at the same level in these graphs indicates no interaction. The DLS data for calbindin $D_{9k}$ variants (M0, M11 and M56) support the fluorescence data since their size values are within the same range as the control values in HEPES buffer. Contrary to these findings regarding calbindin, the DLS data does not support the fluorescence data for all monellin variants ((-2), (+2) and (+8)). In accordance with the DLS data, evidence of aggregate formation in every monellin sample except for S2 in combination with (-2) and S3 in combination with (+2) were found.

Results from a second screening with ANS and a lower concentration of (+8) are shown in Figure 5. These graphs give an indication of an interaction between the NPs and the protein ($I_{F\ total} < I_{F\ protein} + I_{F\ NP}$ (green < blue + red)) and was the groundwork for the additional screening measuring different concentrations of (+8). The DLS data from this screening is presented in Table 2. The values reported in Table 2 indicate fewer aggregate formations than in Table 1.

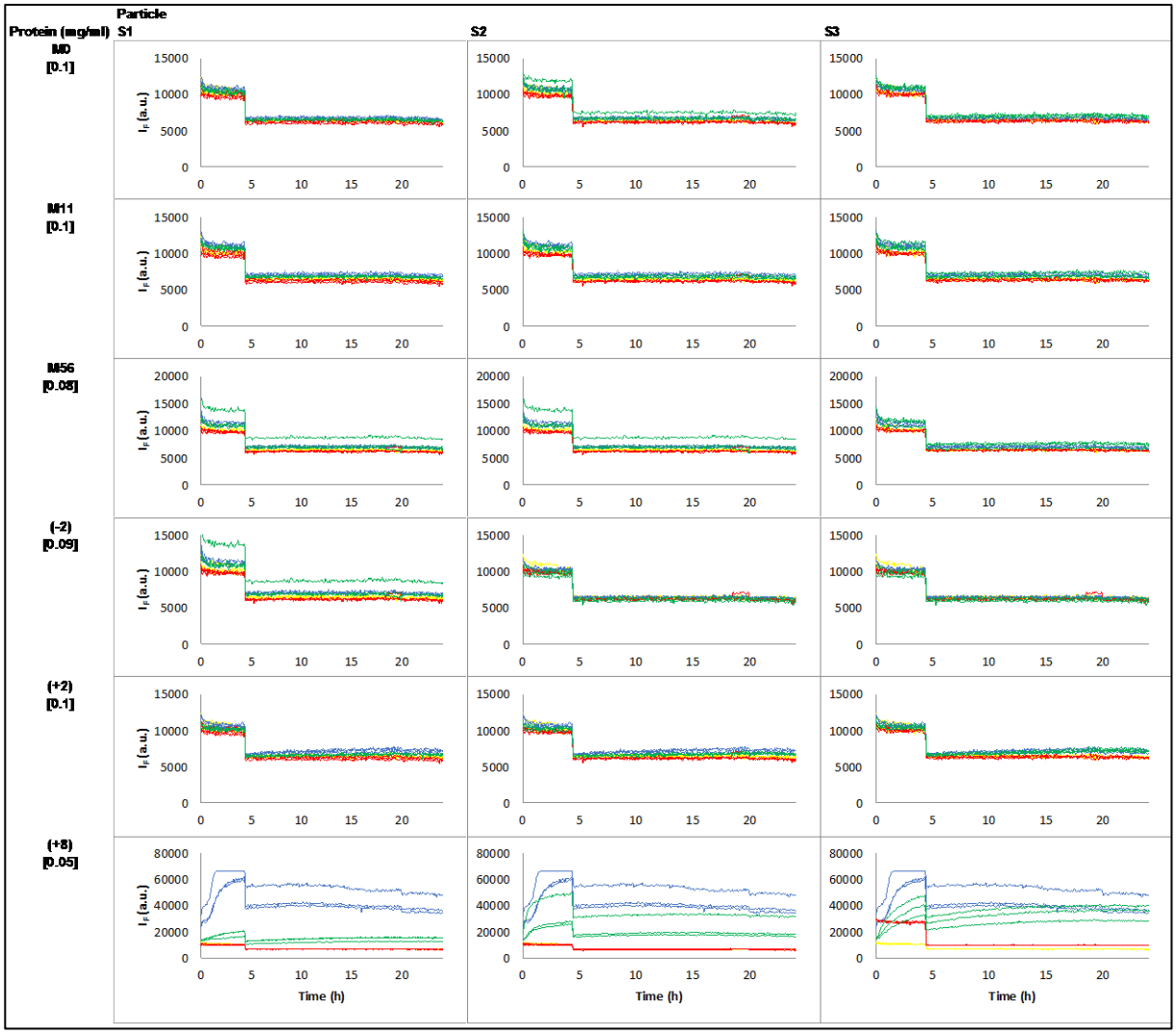


*Figure 4. Raw data of full screening with ANS. Yellow = ANS, blue = Protein + ANS, red = ANS + NP, green = ANS + NP + Protein. The big shift in fluorescence intensity right before 5 h is due to changed gain settings.*

*Table 1. NP sizes measured by DLS for first ANS full screening.*

| **ANS 1** | **S1** | **S2** | **S3** |
|---|---|---|---|
| | **Size (nm) ± Std dev** | **Size (nm) ± Std dev** | **Size (nm) ± Std dev** |
| In HEPES buffer | 22.8 ± 1.3 | 35.5 ± 0.8 | 106.3 ± 9.4 |
| + Fluorophore | 24.3* ± 1.2 | 36.3 ± 0.8 | 109.5 ± 5.4 |
| With Calbindin $D_{9k}$: | | | |
| **M0** | 25.8 ± 0.9 | 37.2 ± 1.8 | 108.4 ± 1.1 |
| **M11** | 27.3 ± 3.1 | 38.4 ± 0.3 | 111.2 ± 3.8 |
| **M56** | 26.1 ± 1.1 | 37.9 ± 0.7 | 108.3 ± 1.8 |

| | | | |
|---|---|---|---|
| With Monellin: | | | |
| **(-2)** | ~ 29.3 ± 1.9 and 317.4 ± 59.9 | 38.6 ± 0.7 | ~ 75 and 300 |
| **(+2)** | ~ 58.5 and 127.0 ± 27.6 | 92.8 ± 0.4 | 111.7 ± 5.3 |
| **(+8)** | ~ 48.0 ± 8.9 and 473.5 ± 51.1 | ~ 42.2 ± 3.2 and 352.7 ± 20.2 | 152.3 ± 7.7 |

*Outlier excluded

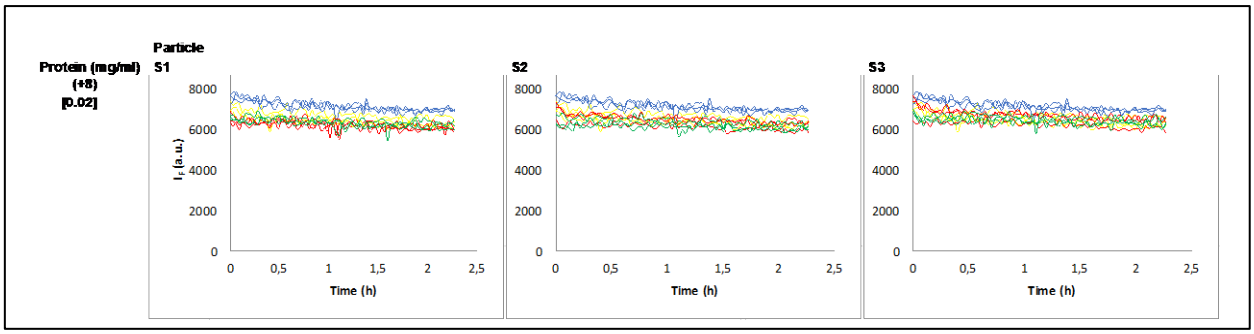


*Figure 5. Raw data of second screening with ANS and (+8) mutation of Monellin. Yellow = ANS, blue = Protein + ANS, red = ANS + NP, green = ANS + NP + Protein.*

*Table 2. NP sizes measured by DLS for second screening with ANS and (+8) mutation of Monellin.*

| **ANS 2** | **S1** | **S2** | **S3** |
|---|---|---|---|
| | **Size (nm) ± Std dev** | **Size (nm) ± Std dev** | **Size (nm) ± Std dev** |
| In HEPES buffer | 22.8 ± 1.3 | 35.5 ± 0.8 | 106.3 ± 9.4 |
| + Fluorophore | 29.1 ± 2.3 | 34.8 ± 0.5 | 91.3 ± 18.6 |
| With Calbindin $D_{9k}$: | | | |
| **M0** | 24.1 ± 2.3 | 35.1 ± 1.0 | 117.1 ± 7.3 |
| **M11** | 26.5 ± 0.4 | 35.7 ± 0.6 | 112.3 ± 1.4 |
| **M56** | 24.3 ± 0.7 | 35.7 ± 0.5 | 109.8 ± 1.7 |
| With Monellin: | | | |
| **(-2)** | 26.7 ± 1.2 | 34.9 ± 1.4 | 122.3 ± 12.5 |
| **(+2)** | 42.2 ± 4.8 | 66.5 ± 12.9 | 111.8 ± 3.8 |
| **(+8)** | ~ 27.5 ± 2.1 and 157.0 ± 12.1 | ~ 47.9 ± 1.1 and 237.6 ± 30.7 | 117.0 ± 1.9 |

*4.2 Fluorescence measurements with NR*

Results from fluorescence measurements with NR are shown in Figure 6, and DLS data from the same test run is presented in Table 3. In comparison, the DLS data from the NR screening show similar results as in ANS2 (Table 2). However, the fluorescence data is difficult to interpret because of the unexpected behavior of some samples (e.g. a buffer control in yellow and a NP control in red). Between the time 0-2 hours, indication of interaction for S2 and S3 can be observed (if outliers are ignored) while after two hours and onwards any difference between the samples is difficult to detect. There is a distinct difference between S1 and the other two NPs where, disregarding the outlier, the NP control value in red is very low. The relationship between the samples can be estimated as $I_{F\ total} = I_{F\ protein} + I_{F\ NP}$ which

demonstrates a no protein adsorption scenario. Regarding the larger size NPs, S2 and S3, the NP control value in red is at a higher fluorescence intensity level which demonstrate protein-NP interaction due to the relationship $I_{F\ total} < I_{F\ protein} + I_{F\ NP}$. Interaction between calbindin $D_{9k}$ M0 and the three NPs is particularly prominent during the first 90-120 minutes. In addition, the results in Figure 6 show that the time course of interaction between NR and Calbindin $D_{9k}$ variants is faster in the absence of NPs, indicated by the blue graphs that are initially steeper than the green ones.

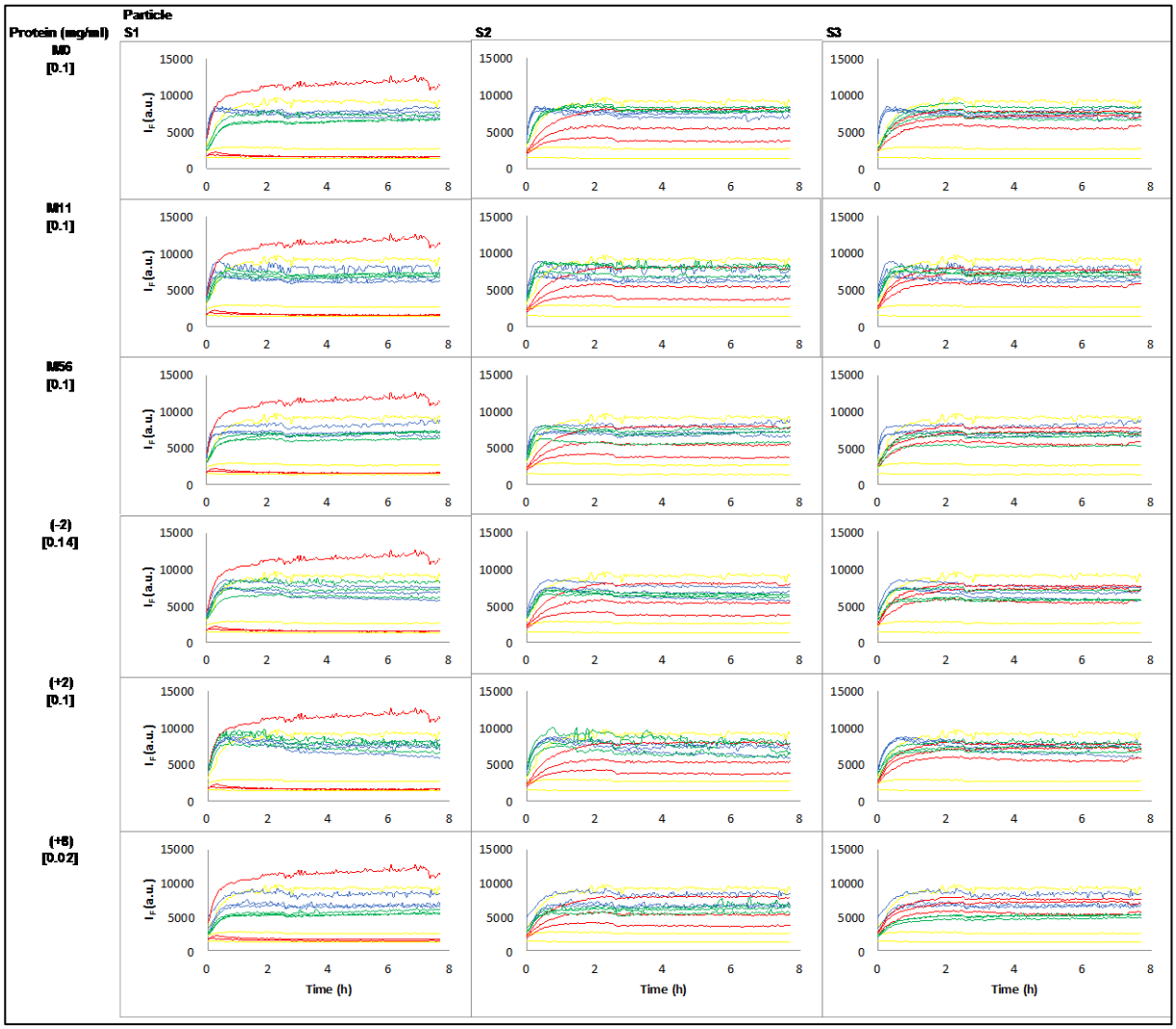


*Figure 6. Screening raw data of full screening with NR. Yellow = NR, blue = Protein + NR, red = NR + NP, green = NR + NP + Protein.*

*Table 3. NP sizes measured by DLS for NR full screening.*

| NR | **S1** | **S2** | **S3** |
|---|---|---|---|
| | **Size (nm) ± Std dev** | **Size (nm) ± Std dev** | **Size (nm) ± Std dev** |
| In HEPES buffer | 22.8 ± 1.3 | 35.3 ± 0.8 | 106.3 ± 9.4 |
| + Fluorophore | 43.1 ± 16.7 | 37.1 ± 1.6 | 119.9 ± 1.7 |
| With Calbindin $D_{9k}$: | | | |
| **M0** | 22.7 ± 0.7 | 35.5 ± 0.2 | 115.3 ± 3.9 |
| **M11** | 22.2 ± 0.8 | 36.4 ± 0.6 | 113.9 ± 2.5 |
| **M56** | 23.6 ± 0.7 | 39.2 ± 0.5 | 113.2 ± 4.0 |
| With Monellin: | | | |
| **(-2)** | 55.3 ± 56.5 | 34.8 ± 1.1 | 117.9 ± 2.4 |
| **(+2)** | 44.8 ± 4.9 | 49.6 ± 3.5 | 115.7 ± 4.1 |
| **(+8)** | ~ 26 and 188 | 51.1 ± 9.1 | 120.8 ± 3.3 |

*4.3 ANS measurements on different (+8) concentrations*

In Figure 7, 8 and 9 are the results from the ANS screening on S1, S2 and S3 respectively in combination with different concentrations of (+8). ANS+(+8) in blue correspond to $I_{F\ protein}$, S1+ANS in orange correspond to $I_{F\ NP}$ and S1+ANS+(+8) in grey correspond to $I_{F\ total}$. The concentrations of NPs and ANS are constant, only the protein concentration is modified. Thus, the graphs show that the protein concentration influence the ability of ANS to bind the protein. Furthermore, it seems that the larger the size of the NP the smaller the concentration limit, since $I_{F\ total}$ continues to be higher compared to $I_{F\ protein}$ for S2 and S3 until the (+8) concentration of 0.04 mg/ml, but only until 0.06 mg/ml for S1. Essentially, the relationship between the samples can be set as $I_{F\ total} > I_{F\ protein} + I_{F\ NP}$ which point out a protein adsorption scenario and possibly a conformational change of the protein. DLS data from this test run is shown in Table 4.

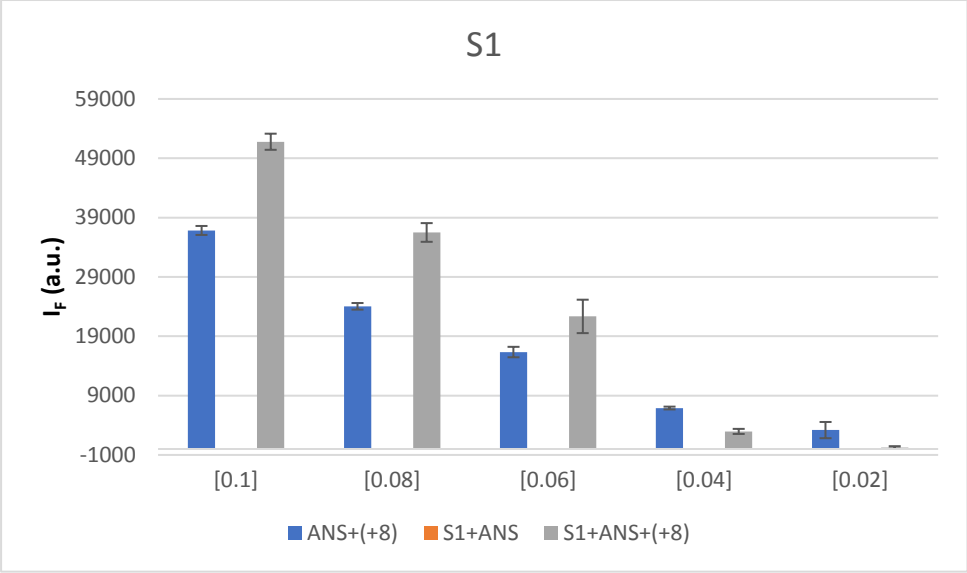


*Figure 7. Screening with ANS on S1 in combination with different concentrations of (+8). Concentration values are in mg/ml. ANS+(+8) = $I_{F\ protein}$, S1+ANS = $I_{F\ NP}$ and S1+ANS+(+8) = $I_{F\ total}$.*

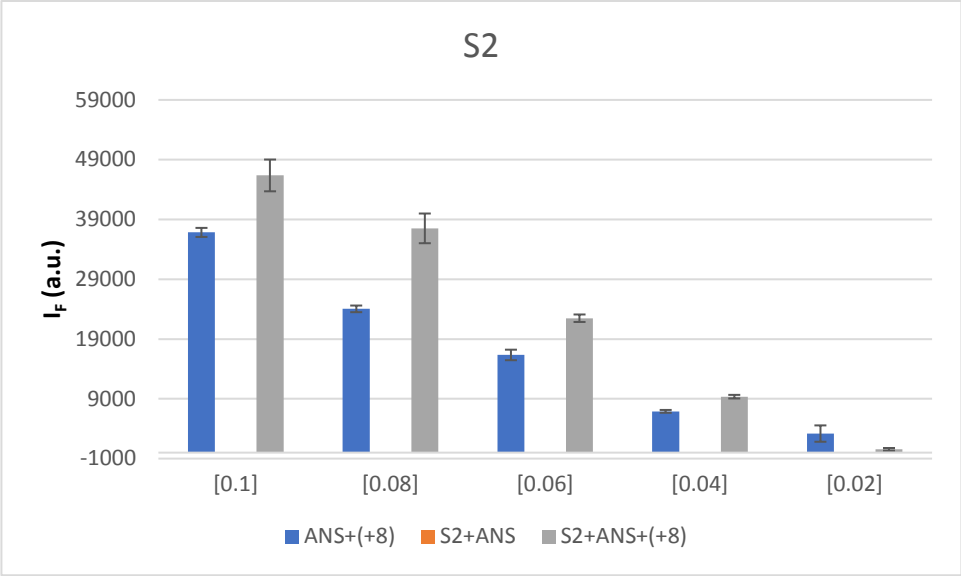


*Figure 8. Screening on S2 with ANS in combination with different concentrations of (+8). Concentration values are in mg/ml. ANS+(+8) = $I_{F\ protein}$, S2+ANS = $I_{F\ NP}$ and S1+ANS+(+8) = $I_{F\ total}$*

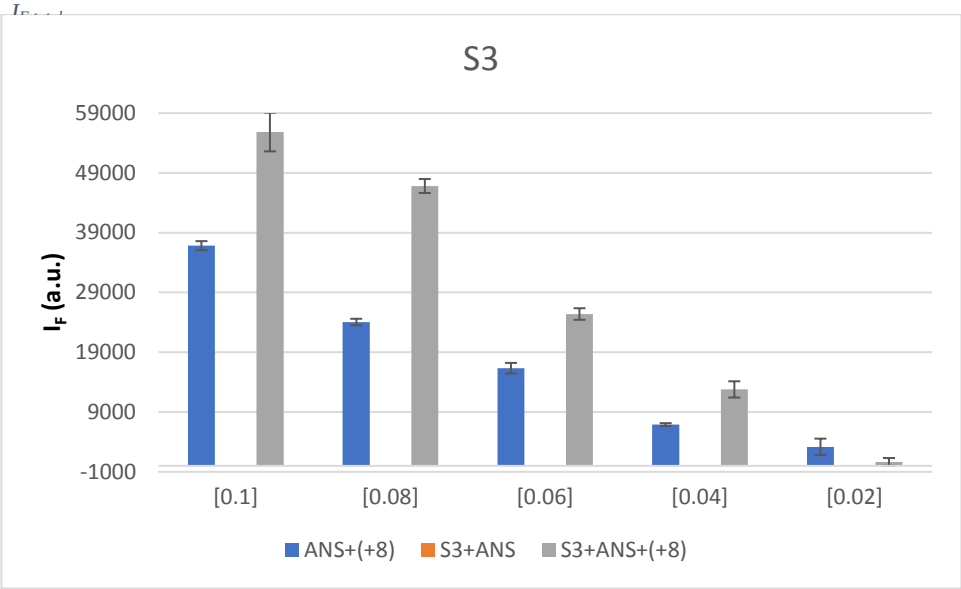


*Figure 9. Screening on S3 with ANS in combination with different concentrations of (+8). Concentration values are in mg/ml. ANS+(+8) = $I_{F\ protein}$, S3+ANS = $I_{F\ NP}$ and S1+ANS+(+8) = $I_{F\ total}$*

*Table 4. NP sizes measured by DLS for ANS full screening of S1, S2 and S3 in combination with different concentrations of Monellin (+8).*

| **ANS 3** | **S1** | **S2** | **S3** |
|---|---|---|---|
| | **Size (nm) ± Std dev** | **Size (nm) ± Std dev** | **Size (nm) ± Std dev** |
| In HEPES buffer | 22.8 ± 1.3 | 35.3 ± 0.8 | 106.3 ± 9.4 |
| + Fluorophore | 46.9 ± 13.1 | 61.3 ± 11.3 | 103.6 ± 9.2 |
| With Monellin (+8): | | | |
| **[0.1]** | 49.1 ± 6.6 | 39.7 ± 4.5 | 109.0* |
| **[0.08]** | 43.9 ± 5.3 | 39.0* | Agg[1] |
| **[0.06]** | Agg[1] | Agg[1] | 161.7 ± 10.4 |
| **[0.04]** | 53.1* | Agg[1] | 126.8 ± 8.7 |
| **[0.02]** | 45.1 ± 9.1 | 46.2 ± 7.4 | 109.7 ± 3.2 |

[1]Aggregates formed
*Outliers excluded

## 5. Discussion

The aim of this study was to explore the interactions between three different mutations of the two proteins calbindin $D_{9k}$ and monellin with silica NPs of three different sizes. The two fluorophores used in the fluorescence measurements both report on hydrophobicity and not charge. Silica NPs mainly have a hydrophilic surface and, consequently, none of the fluorophores adsorb to the NP surface. Thus, possible scenarios for this study are limited to section A as described in Figure 1.

In this study methods that may be applicable to other proteins and NPs were used. Results obtained from this series of experiments indicate that further experiments with a similar methodology should be pursued. The initial ANS screenings and their associated DLS data show no interaction between calbindin $D_{9k}$ variants and NPs, illustrated by scenario 3a in Figure 1. Calbindin $D_{9k}$ is known to be an inert protein hence not surprisingly non-interactive. All the mutants (M0, M11 and M56) were negatively charged. Silica NPs also have a negative surface charge leading to the assumption that repulsion rather than attraction between the two is likely, which is seen in the results. Monellin mutants (-2) and (+2) in combination with S1, S2 and S3 indicate no interaction from ANS screening results. Their corresponding DLS data however, does not fully support this statement. DLS data for NP in combination with monellin indicate that NP aggregates seem to have been formed while NP in combination with calbindin appear to have colloidal stability. This is possibly due to the ability to adsorb to the NP surface for monellin variants and not calbindin $D_{9k}$ variants. The more homogenous a solution is the more reliable DLS measurements on that solution will be. It is conceivable that the non-homogeneity of the samples had an impact on the DLS results. The ANS screening results of monellin (+8) indicate interaction *per* scenario 1a in Figure 1. The relatively high positive charge of (+8) make it plausible that an electrostatic binding may naturally occur to the negatively charged NP and is consistent with the results.

The fluorescence measurements with NR are more difficult to interpret. The DLS data were relatively steady, indicating the same protein-NP interactive outcome as for ANS measurements. However, NR and silica NPs seem to be less compatible than ANS and silica, a finding supported by the larger number of outliers for NR screenings. Disregarding the outliers, the smaller S1 show no interaction with proteins while S2 and S3 appear to adsorb protein. Contrary to what was expected, the results indicate that S2 and S3 adsorb the fluorophore which means that the interaction possibilities presented in section B, Figure 1 should be considered. However, more experiments are needed to confirm these results. The

time course of interaction between NR and calbindin $D_{9k}$ mutations is faster in the absence of NPs. This could validate the adsorption scenario because of possible steric hindrance, occurring as consequence of the protein-NP adsorption, which would slow down the binding process between NR and either M0, M11 or M56.

The ANS measurements with the monellin (+8) concentration scale from 0.02 mg/ml to 0.1 mg/ml was designed to consider if the protein-NP adsorption had a protein concentration dependence which, given the results, seems to be the case. The outcome of this test run is an $I_{F\ total} > I_{F\ protein} + I_{F\ NP}$ relationship, as described as scenario 2a of Figure 1. This suggests a conformational change of the protein taking place as the binding to the NP develop. This however is difficult to confirm without further investigation. Furthermore, the DLS data show that several unwanted aggregates were formed. The (+8) mutant may be unstable but it also proves that further experiments are necessary before definitive conclusions can be drawn.

If a structural change of a protein occurs, its function will most likely also change. The long-term ambition of research in this field is to obtain knowledge about specific protein-NP combinations to such a degree that a possible conformational change of protein structure, due to NP adsorption, and its significance *in vivo* is known. Fundamental research will, in addition to adding to methodological and study design knowledge, increase the understanding of specific protein-NP combinations and their interactions, which in turn will improve the predictions for similar combinations in the future.

## 6. Conclusions

The main findings of this experiment show that the silica NPs most likely do interact with monellin. The (+8) variant of monellin is particularly interactive and indicate on protein concentration dependence. The NP size appear to have an impact on the concentration limits for (+8). The results of the experiments also indicate that ANS is a more suitable fluorophore than NR for fluorescence measurements on silica NPs.

## References:


1. Assarsson, A. (2014). *Adding charge*. 1st ed. Lund: Department of Biochemistry and Structural Biology, Lund University.
2. Daintith, J. (2008). *A dictionary of chemistry*. 1st ed. New York: Oxford University Press.
3. Huang, R., Carney, R., Stellacci, F. and Lau, B. (2013). Protein–nanoparticle interactions: the effects of surface compositional and structural heterogeneity are scale dependent. *Nanoscale*, 5(15), p.6928.
4. Lindsay, S. (2010). *Introduction to nanoscience*. 1st ed. Oxford: Oxford University Press.
5. Lundqvist, M., Nygren, P., Jonsson, B. and Broo, K. (2006). Induction of Structure and Function in a Designed Peptide upon Adsorption on a Silica Nanoparticle. *Angewandte Chemie International Edition*, 45(48), pp.8169-8173.
6. Lundqvist, M., Sethson, I. and Jonsson, B. (2004). Protein Adsorption onto Silica Nanoparticles: Conformational Changes Depend on the Particles' Curvature and the Protein Stability. *Langmuir*, 20(24), pp.10639-10647.
7. Mosby's dictionary of medicine, nursing & health professions. (2006). 7th ed. St. Louis, Mo.: Mosby Elsevier.

8. Nasir, I., Fatih, W., Svensson, A., Radu, D., Linse, S., Cabaleiro Lago, C. and Lundqvist, M. (2015). High Throughput Screening Method to Explore Protein Interactions with Nanoparticles. *PLOS ONE*, 10(8), p.e0136687.
9. Napierska, D., Thomassen, L., Lison, D., Martens, J. and Hoet, P. (2010). The nanosilica hazard: another variable entity. *Particle and Fibre Toxicology*, 7(1), p.39.
10. O'Connell, D., Bauer, M., Linse, S. and Cahill, D. (2011). Probing Calmodulin Protein–Protein Interactions Using High-Content Protein Arrays. *Methods in Molecular Biology*, pp.289-303.
11. Rauscher, H., Sokull-Klüttgen, B., Stamm, H., 2013. The European Commission's recommendation on the definition of nanomaterial makes an impact. Nanotoxicology 7, 1195–1197. doi:10.3109/17435390.2012.724724
12. Rosi, N. and Mirkin, C. (2005). Nanostructures in Biodiagnostics. *ChemInform*, 36(28).
13. Shang, L., Nienhaus, K. and Nienhaus, G. (2014). Engineered nanoparticles interacting with cells: size matters. *Journal of Nanobiotechnology*, 12(1), p.5.

# Appendix

| ANS | 1 | 2 | 3 | 4 | 5 | 6 | 7 | 8 | 9 | 10 | 11 | 12 |
|---|---|---|---|---|---|---|---|---|---|---|---|---|
| A | ANS | ANS | ANS | ANS+M0 | ANS+M0 | ANS+M0 | ANS+M11 | ANS+M11 | ANS+M11 | ANS+M56 | ANS+M56 | ANS+M56 |
| B | S1+ANS | S1+ANS | S1+ANS | S1+ANS+M0 | S1+ANS+M0 | S1+ANS+M0 | S1+ANS+M11 | S1+ANS+M11 | S1+ANS+M11 | S1+ANS+M56 | S1+ANS+M56 | S1+ANS+M56 |
| C | S2+ANS | S2+ANS | S2+ANS | S2+ANS+M0 | S2+ANS+M0 | S2+ANS+M0 | S2+ANS+M11 | S2+ANS+M11 | S2+ANS+M11 | S2+ANS+M56 | S2+ANS+M56 | S2+ANS+M56 |
| D | S3+ANS | S3+ANS | S3+ANS | S3+ANS+M0 | S3+ANS+M0 | S3+ANS+M0 | S3+ANS+M11 | S3+ANS+M11 | S3+ANS+M11 | S3+ANS+M56 | S3+ANS+M56 | S3+ANS+M56 |
| E | | | | ANS+(-2) | ANS+(-2) | ANS+(-2) | ANS+(+2) | ANS+(+2) | ANS+(+2) | ANS+(+8) | ANS+(+8) | ANS+(+8) |
| F | | | | S1+ANS+(-2) | S1+ANS+(-2) | S1+ANS+(-2) | S1+ANS+(+2) | S1+ANS+(+2) | S1+ANS+(+2) | S1+ANS+(+8) | S1+ANS+(+8) | S1+ANS+(+8) |
| G | | | | S2+ANS+(-2) | S2+ANS+(-2) | S2+ANS+(-2) | S2+ANS+(+2) | S2+ANS+(+2) | S2+ANS+(+2) | S2+ANS+(+8) | S2+ANS+(+8) | S2+ANS+(+8) |
| H | | | | S3+ANS+(-2) | S3+ANS+(-2) | S3+ANS+(-2) | S3+ANS+(+2) | S3+ANS+(+2) | S3+ANS+(+2) | S3+ANS+(+8) | S3+ANS+(+8) | S3+ANS+(+8) |

*Figure 10. Plate plan for ANS full screening.*

| NR | 1 | 2 | 3 | 4 | 5 | 6 | 7 | 8 | 9 | 10 | 11 | 12 |
|---|---|---|---|---|---|---|---|---|---|---|---|---|
| A | NR | NR | NR | NR+M0 | NR+M0 | NR+M0 | NR+M11 | NR+M11 | NR+M11 | NR+M56 | NR+M56 | NR+M56 |
| B | S1+NR | S1+NR | S1+NR | S1+NR+M0 | S1+NR+M0 | S1+NR+M0 | S1+NR+M11 | S1+NR+M11 | S1+NR+M11 | S1+NR+M56 | S1+NR+M56 | S1+NR+M56 |
| C | S2+NR | S2+NR | S2+NR | S2+NR+M0 | S2+NR+M0 | S2+NR+M0 | S2+NR+M11 | S2+NR+M11 | S2+NR+M11 | S2+NR+M56 | S2+NR+M56 | S2+NR+M56 |
| D | S3+NR | S3+NR | S3+NR | S3+NR+M0 | S3+NR+M0 | S3+NR+M0 | S3+NR+M11 | S3+NR+M11 | S3+NR+M11 | S3+NR+M56 | S3+NR+M56 | S3+NR+M56 |
| E | | | | NR+(-2) | NR+(-2) | NR+(-2) | NR+(+2) | NR+(+2) | NR+(+2) | NR+(+8) | NR+(+8) | NR+(+8) |
| F | | | | S1+NR+(-2) | S1+NR+(-2) | S1+NR+(-2) | S1+NR+(+2) | S1+NR+(+2) | S1+NR+(+2) | S1+NR+(+8) | S1+NR+(+8) | S1+NR+(+8) |
| G | | | | S2+NR+(-2) | S2+NR+(-2) | S2+NR+(-2) | S2+NR+(+2) | S2+NR+(+2) | S2+NR+(+2) | S2+NR+(+8) | S2+NR+(+8) | S2+NR+(+8) |
| H | | | | S3+NR+(-2) | S3+NR+(-2) | S3+NR+(-2) | S3+NR+(+2) | S3+NR+(+2) | S3+NR+(+2) | S3+NR+(+8) | S3+NR+(+8) | S3+NR+(+8) |

*Figure 11. Plate plan for NR full screening.*

| ANS+(+8) | 1 | 2 | 3 | 4 | 5 | 6 | 7 | 8 | 9 | 10 | 11 | 12 |
|---|---|---|---|---|---|---|---|---|---|---|---|---|
| A | ANS | ANS | ANS | ANS+[0.1] | ANS+[0.1] | ANS+[0.1] | ANS+[0.08] | ANS+[0.08] | ANS+[0.08] | | | |
| B | S1+ANS | S1+ANS | S1+ANS | S1+ANS+[0.1] | S1+ANS+[[0.1]] | S1+ANS+[0.1] | S1+ANS+[0.08] | S1+ANS+[0.08] | S1+ANS+[0.08] | | | |
| C | S2+ANS | S2+ANS | S2+ANS | S2+ANS+[0.1] | S2+ANS+[0.1] | S2+ANS+[0.1] | S2+ANS+[0.08] | S2+ANS+[0.08] | S2+ANS+[0.08] | | | |
| D | S3+ANS | S3+ANS | S3+ANS | S3+ANS+[0.1] | S3+ANS+[0.1] | S3+ANS+[0.1] | S3+ANS+[0.08] | S3+ANS+[0.08] | S3+ANS+[0.08] | | | |
| E | ANS+[0.06] | ANS+[0.06] | ANS+[0.06] | ANS+[0.04] | ANS+[0.04] | ANS+[0.04] | ANS+[0.02] | ANS+[0.02] | ANS+[0.02] | | | |
| F | S1+ANS+[0.06] | S1+ANS+[0.06] | S1+ANS+[0.06] | S1+ANS+[0.04] | S1+ANS+[0.04] | S1+ANS+[0.04] | S1+ANS+[0.02] | S1+ANS+[0.02] | S1+ANS+[0.02] | | | |
| G | S2+ANS+[0.06] | S2+ANS+[0.06] | S2+ANS+[0.06] | S2+ANS+[0.04] | S2+ANS+[0.04] | S2+ANS+[0.04] | S2+ANS+[0.02] | S2+ANS+[0.02] | S2+ANS+[0.02] | | | |
| H | S3+ANS+[0.06] | S3+ANS+[0.06] | S3+ANS+[0.06] | S3+ANS+[0.04] | S3+ANS+[0.04] | S3+ANS+[0.04] | S3+ANS+[0.02] | S3+ANS+[0.02] | S3+ANS+[0.02] | | | |

*Figure 12. Plate plan for ANS screening with different concentrations of (+8).*